Structure and hydrogen dynamics of pure and Ti-doped sodium alanate

Jorge Íñiguez,[1,2] T. Yildirim,[1] T. J. Udovic,[1] M. Sulic,[3] and C. M. Jensen[3]

[1]*NIST Center for Neutron Research, National Institute of Standards and Technology, Gaithersburg, Maryland 20899, USA*
[2]*Department of Materials Science and Engineering, University of Maryland, College Park, Maryland 20742, USA*
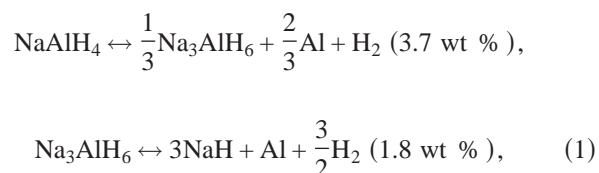[3]*Department of Chemistry, University of Hawaii, Honolulu, Hawaii 96822, USA*

We have studied the structure, energetics, and dynamics of pure and Ti-doped sodium alanate ($NaAlH_4$), focusing on the possibility of substitutional Ti doping in the bulk. Our *ab initio* calculations reproduce well the measured neutron inelastic scattering spectrum, which exhibits surprisingly strong and sharp two-phonon features. The calculations also reveal that substitutional Ti doping is energetically possible, and imply that Ti prefers to substitute for Na and is a powerful hydrogen attractor that facilitates multiple Al-H bond breaking. Our results hint at ways of improving the hydrogen dynamics and storage capacity of the alanates.

Developing safe, cost-effective, and practical means of storing hydrogen is crucial for the advancement of hydrogen and fuel cell technologies. Presently, there are three generic routes for the solid-state storage of hydrogen: (i) physisorption as in many porous carbon and zeolite materials; (ii) chemisorption as in metal hydrides; and (iii) chemical reaction such as in complex metal hydrides. Among the type (iii) materials, sodium alanate ($NaAlH_4$) has received considerable attention because of its high hydrogen weight capacity and low cost. The release of hydrogen from $NaAlH_4$ occurs via a two-step reaction

$$NaAlH_4 \leftrightarrow \frac{1}{3}Na_3AlH_6 + \frac{2}{3}Al + H_2 \text{ (3.7 wt \%)},$$

$$Na_3AlH_6 \leftrightarrow 3NaH + Al + \frac{3}{2}H_2 \text{ (1.8 wt \%)}, \qquad (1)$$

yielding a total of 5.5 wt % hydrogen. It was recently reported that a few percent of Ti doping in $NaAlH_4$ renders accelerated and reversible hydrogen release under moderate conditions.[1] In spite of the extensive investigations of Ti-doped $NaAlH_4$ that have resulted, little is known about the mechanism by which Ti enhances the cycling kinetics of hydrogen.[2,3] In fact, even the location of the Ti atoms remains unclear. While it is widely believed that they reside on the surface of the material,[4] the possibility that Ti is substituted for Na has also been suggested,[5] but convincing experimental or theoretical evidence is still lacking.

Here we present first-principles total energy and dynamics calculations of pure and Ti-doped sodium alanates, focusing on the possibility of substitutional Ti doping in the bulk. Along with the calculations, we report neutron inelastic scattering (NIS) measurements of the phonon density of states, which allow us to validate our computational approach. We succeed in characterizing the main features in the observed spectrum, which displays surprisingly strong two-phonon contributions. Furthermore, the calculations show that it is most energetically favorable for Ti to substitute for Na, breaking several Al-H bonds in its vicinity. We also find that Ti-doped $NaAlH_4$ can accommodate extra hydrogen near the

dopant. In addition, we examine the effect of the Ti dopants on the vibrational spectrum of neighboring AlH_4 groups, which could allow probing the Ti location in doped samples using high resolution spectroscopic techniques.

Three powder samples were investigated: pure $NaAlH_4$, 2% Ti-doped $NaAlH_4$, and Na_3AlH_6. $NaAlH_4$ was prepared as described in Ref. 6. $NaAlH_4$ was doped with 2 mol percent TiF_3 through mechanical milling according to standard procedure.[7] Na_3AlH_6 was synthesized and purified by the method of Huot *et al.*[8] The NIS measurements were performed using the filter analyzer neutron spectrometer at the NIST Center for Neutron Research (Gaithersburg, Maryland)[9] under conditions that provided energy resolutions of 2-4.5 % in the range probed.

The calculations were performed within the plane-wave implementation of the generalized gradient approximation[10] to density functional theory in the ABINIT package.[11] We used Troullier-Martins pseudopotentials[12,13] treating the following electronic states as valence: $3d$ and $4s$ of Ti, $3s$ and $3p$ of Al, $3s$ of Na, and $1s$ of H. We carefully tested the convergence of our calculations with respect to the plane-wave cutoff and k-point mesh. For example, for the Ti-doped alanate supercells (containing 96 atoms) we used a cutoff of 1250 eV and a $3 \times 3 \times 2$ k-point mesh. The phonon spectrum of the pure compound was computed using density functional perturbation theory[14] as implemented in ABINIT. We calculated the phonons corresponding to two $2 \times 2 \times 2$ q-point grids. An interpolation scheme was then used so that the powder-averaged NIS phonon spectra were computed for a $4 \times 4 \times 4$ q-point grid within the incoherent approximation.[15]

We first optimized the tetragonal $NaAlH_4$ and monoclinic Na_3AlH_6 structures. The results, summarized in Table I, agree reasonably well with previous x-ray[16] and neutron[17,18] studies. For example, the reported $NaAlH_4$ lattice parameters (at 8 K)[17] are 4.98 and 11.15 Å, respectively, while we obtain 4.98 and 11.05 Å. The reported H position (0.237, 0.384, 0.547) is in good agreement with our result.

We also calculated the energy change associated with the two reactions in Eq. (1) and obtained, respectively, 24 and 42 kJ/mol of H_2 released, compared to the experimental enthalpies of reaction of 37 and 47 kJ/mol.[19] The agreement is reasonably good taking into account (i) we cannot directly

TABLE I. Calculated structural parameters of $NaAlH_4$ and Na_3AlH_6.

$NaAlH_4$	$I4_1/a$	$a=4.98$ Å,	$c=11.05$ Å	
Atom	Wyc.	x	y	z
Al	4b	0	1/4	5/8
Na	4a	0	1/4	1/8
H	16f	0.2335	0.3918	0.5439

Na_3AlH_6	$P2_1/n$			
$a=5.33$ Å,	$b=5.53$ Å,	$c=7.68$,	$\beta=90.103°$	
Atom	Wyc.	x	y	z
Al	2a	0	0	0
Na	2b	0	0	1/2
Na	4e	0.9897	0.4532	0.2535
H	4e	0.1000	0.0481	0.2164
H	4e	0.2281	0.3307	0.5437
H	4e	0.1608	0.2673	0.9366

compare our energy differences with the experimental enthalpies (because we do not consider contributions from vibrational entropies, etc.) and (ii) the error associated with our first-principles approach is of the order of $5-10$ kJ/mol. This error is estimated from the error in the calculated cohesive energies of individual compounds; e.g., we get $E_{coh}=4.53$ eV for the H_2 molecule, while the experimental value is 4.49 eV.

The vibrational spectrum of $NaAlH_4$ is shown in Fig. 1. The calculated one-phonon spectrum does not reproduce several experimentally observed features. Yet, including two-phonon processes yields results that are in excellent agreement with the observed spectrum. [We also obtained very good agreement between theory and experiment for the phonon spectrum of Na_3AlH_6 (not shown here).] The two-phonon peak in Fig. 1 comes from the combination of one-phonon processes associated with the peaks around 55 and
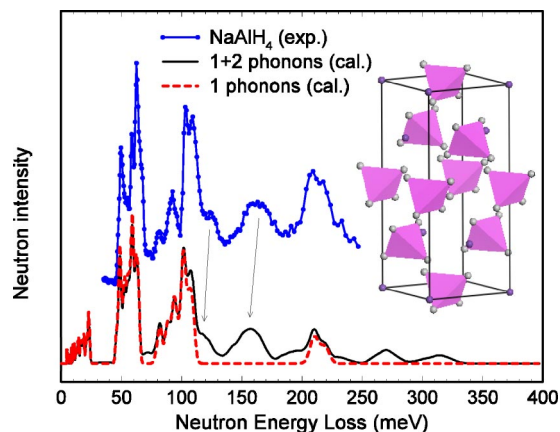

FIG. 1. (Color online) Measured (top) and calculated (bottom) NIS spectra of $NaAlH_4$. The calculated 1 and $1+2$ phonon contributions are shown. The structure of $NaAlH_4$ is shown in the inset; grey tetrahedra represent AlH_4 units. The measurements were performed at 8 K.
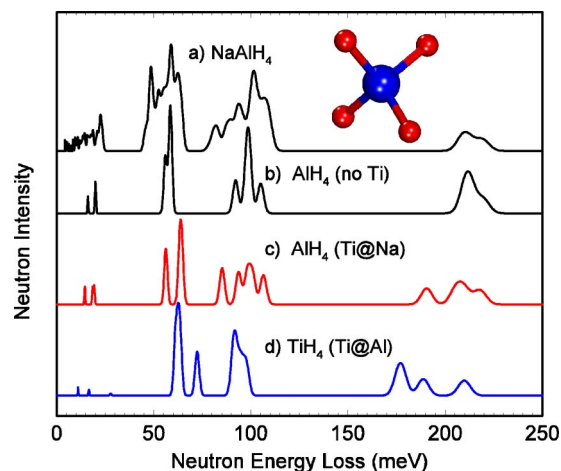

FIG. 2. (Color online) Calculated one-phonon NIS spectra for (a) $NaAlH_4$ and for a single MH_4 tetrahedron for various cases: (b) pure alanate, (c) Ti→Na, and (d) Ti→Al.

100 meV. The AlH_4 units seem to be weakly interacting, which results in sharp one-phonon peaks and relatively sharp two-phonon features as well. These latter features are similar to overtones observed in Raman or IR molecular spectra. Such strong multiphonon contributions are unusual, but they seem to be typical of materials with MH_x groups, where M is a metal atom.[20]

The nature of the different phonon bands in Fig. 1 can be determined by computing the modes of the individual AlH_4 groups in the crystalline matrix. (Note that the NIS spectrum is dominated by hydrogen modes.[15]) The dynamical matrix of the AlH_4 group is constructed using the the finite displacement technique[21] and then diagonalized. As shown in Fig. 2(b), we obtain four distinct groups of modes that correspond to the largest features in the one-phonon spectrum of Fig. 2(a). Inspection of the eigenvectors allows the characterization of the modes. The lowest-frequency modes are AlH_4 translations, while the peak above 200 meV consists of stretching modes of the AlH_4 tetrahedron. The modes in the two intermediate sets are a mixture of rotations and stretches.

Now we extend our calculations to investigate the possibility of substitutional Ti doping of alanates. First we study whether Ti-doped alanate is energetically stable and, if so, where the Ti dopant goes. From the many substitutional and interstitial doping models that could be tried, we choose two that are experimentally motivated. Doping sodium alanate with solid $TiCl_3$ by dry ball-milling results in the formation of NaCl and partial desorption of $NaAlH_4$, which leads to the formation of aluminum crystallites.[22] Hence, it seems pertinent to study the substitution of Al and Na by Ti. In the following we denote these doping models by "Ti→Al" and "Ti→Na."

We consider supercells containing 16 $NaAlH_4$ formula units, and substitute only one of the Al or Na atoms by Ti. The cohesive energies are obtained as the sum of the individual atom energies minus the energy of the system. The results are given in Table II; E_{coh} of the pure alanate has been chosen as zero energy, so that positive entries indicate greater stability than the pure system.

Note that the results in Table II give minus the energy

TABLE II. Calculated cohesive energies, given in eV and per 96-atom supercell. The result for pure NaAlH$_4$ (231.922 eV) is taken as the zero of energy. E_{coh}^{atom} is the cohesive energy obtained by allowing the atoms to relax but imposing the NaAlH$_4$ relaxed supercell ($V=1095.48$ Å^3); E_{coh}^{atom}(SP) is the same but obtained from spin-polarized calculations; E_{coh}^{full} is the result obtained when allowing both atoms and cell to relax, and V the resulting volume of the 96-atom supercell in Å^3.

System	E_{coh}^{atom}	E_{coh}^{atom}(SP)	E_{coh}^{full}	V
Ti$\rightarrow$Al	0.075	0.408	0.113	1051.10
Ti$\rightarrow$Na	0.911	1.192	1.024	1079.96
Ti$\rightarrow$Na+Na^v	−0.665	0.073	−0.562	1059.52
Ti$\rightarrow$Na+2Na^v	−2.866		−2.778	1059.27
Ti$\rightarrow$Na(H)	1.316			
Ti$\rightarrow$Na+H	1.317			

change in reactions of the form Ti+Na$_{16}$Al$_{16}$H$_{64}\rightarrow$ Al+Na$_{16}$Al$_{15}$TiH$_{64}$, which involve isolated atoms (Ti and Al in this case). These results thus measure the relative stability of pure and doped systems. A positive (and large) entry in the table indicates that, in principle, it is feasible to obtain the doped structure.

We find both Ti$\rightarrow$Na and Ti$\rightarrow$Al are energetically more stable than pure alanate; i.e., the system gains energy by accepting a Ti dopant into the bulk and releasing a Na or Al atom. In addition, Ti$\rightarrow$Na is found to be the most favorable substitution.

The relaxed Ti$\rightarrow$Na structure presents H atoms that come close to the Ti dopant. The shortest Ti-H distance is 2.05 Å, to be compared with the 2.39 Å Na-H distance in the pure system. Consequently, the distance between the hydrogens close to the dopant and their neighboring Al atoms is longer than the Al-H distance in the pure system; we obtain 1.70 and 1.64 Å, respectively. This type of relaxation is to be expected, since Ti has more electrons than Na to share with neighboring hydrogens.

It may seem surprising that Ti$\rightarrow$Na has a higher cohesive energy than Ti$\rightarrow$Al. The typical valences of these atoms certainly suggest otherwise. However, Ti seems to be relatively large for the Al site. In the relaxed Ti$\rightarrow$Al structure we get a Ti-H bond of 1.82 Å, which is much longer than the 1.64 Å Al-H bonds in pure sodium alanate. This size mismatch is the most likely cause for Ti$\rightarrow$Al to be energetically less favorable.

The above results do not change significantly when the electrons are allowed to spin polarize or when we allow both atoms and cell to relax (see E_{coh}^{atom}(SP) and E_{coh}^{full} columns in Table II). The spin-polarized calculations predict the Ti ion retains one unpaired electron in both Ti$\rightarrow$Na and Ti$\rightarrow$Al.

A meaningful modification of the Ti$\rightarrow$Na doping model is to introduce Na vacancies close to the Ti. Na vacancies should yield a more balanced sum of valence charges and have been invoked in the literature to argue that the Ti dopants reside in the bulk of the system.[5] Our results for one and two Na vacancies are in Table II denoted by "Ti$\rightarrow$Na+Na^v" and "Ti$\rightarrow$Na+2Na^v," respectively. When spin polarization is allowed, the Ti$\rightarrow$Na+Na^v structure is found to be more stable than the pure system, but significantly less stable than the doping models considered above. On the other hand, the Ti$\rightarrow$Na+2Na^v structure is predicted to be quite unlikely. All

these calculations preserve the basic NaAlH$_4$ lattice. Hence, our results imply that, if Na vacancies really occur, they will involve strong local distortions of the sodium alanate structure.

The dynamics of the neighboring H atoms could be used as a local probe for the Ti location. However, dynamical calculations for the whole 96-atom supercell are very computationally demanding. Instead, we calculated the vibrational spectrum of a single AlH$_4$ group near the Ti dopant. The results are shown in Fig. 2. In the Ti$\rightarrow$Na case (panel c), the Ti dopant mainly affects the high-frequency modes, i.e., those involving stretching of the AlH$_4$ tetrahedron. All the modes in that group soften. The mode that softens most, approximately from 210 to 190 meV, is dominated by the displacement of H that is closest to the Ti, and essentially corresponds to its oscillation along the Al-Ti direction. This clearly indicates that the presence of Ti could facilitate breaking of the Al-H bond.

In the Ti$\rightarrow$Al case [Fig. 2(d)], the dynamics are modified quite differently since we deal with a TiH$_4$ group. This suggests that, by investigating the phonon spectrum of Ti-doped NaAlH$_4$, one might determine whether Ti dopants go into the bulk of the system and, if so, where they are located. Motivated by this possibility, we measured the phonon spectrum of a 2% Ti-doped sample, but obtained a result essentially identical to that of pure alanate shown in Fig. 1. However, it should be noted that this does not rule out the possibility of substitutional doping in our sample since the amount of Ti is very small, and thus any dopant-induced feature in the spectrum should also be very small and hard to distinguish from the noise. In addition, the NIS spectrum of pure sodium alanate presents significant two-phonon intensity in the 175–200 meV energy range (see Fig. 1), which makes it difficult to identify fine details. Higher resolution spectroscopic measurements, such as Raman scattering, might help elucidate this issue.

The above results suggest that Ti dopants may facilitate the breaking of the Al-H bond. We explored this possibility by moving one H atom to the immediate vicinity of the dopant and then relaxing the system. The resulting structure, which we denote by "Ti$\rightarrow$Na (H)," is considerably more stable than the original Ti$\rightarrow$Na doping model (see E_{coh} in Table II). In fact, we found that it has not one but two H atoms very close to the Ti. The shortest Ti-H distance is
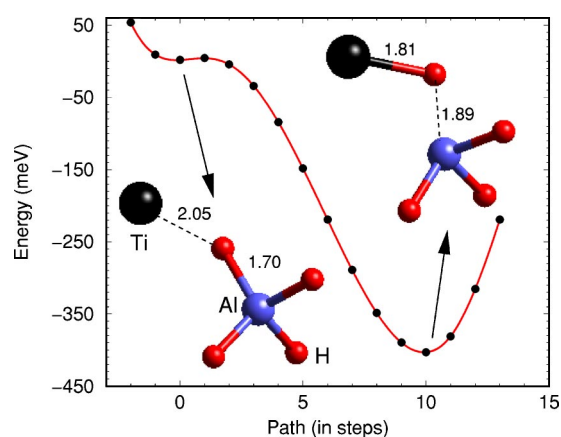
FIG. 3. (Color online) Energy along the path from Ti→Na to Ti→Na (H) structures (see text). Insets show the local structure and bond distances at the two minima. The zero of energy is arbitrary.

1.81 Å, and the corresponding Al-H distance is 1.89 Å, i.e., 0.25 Å longer than in pure $NaAlH_4$. Thus the Ti dopant can indeed induce Al-H bond breaking, a necessary step for H_2 release.

These results indicate that the Ti→Na structure is a local minimum. In Fig. 3 we show the energy change along the transition path leading from Ti→Na to Ti→Na (H). The Ti→Na minimum is very shallow. The calculated energy barrier is around 2.5 meV ≈ 30 K, indicating that Al-H bonds would immediately break in the presence of Ti. Associated with the shallow well is a collective mode of the Ti→Na structure whose frequency can be roughly estimated to be ~80 meV. Yet, the frequency of the AlH_4 mode that we related to the Al-H bond breaking is about 190 meV [see the discussion of Fig. 2(c)]. The reduction from 190 to 80 meV is related to other atomic rearrangements, e.g., the second H coming close to the Ti atom, displacements of the AlH_4 groups, etc.

Along these lines, we also considered a less obvious possibility, namely, that Ti drags extra hydrogens into the system. Table II shows the result for "Ti→Na+H," which corresponds to placing one extra H in the vicinity of the Ti atom. (In the calculation of this cohesive energy, the extra hydrogen was assigned one half of the energy of the H_2 molecule, so that the resulting E_{coh} measures stability against H_2 release.) This structure turns out to be very stable. We find a Ti-H bonding distance of 1.82 Å and several AlH_4 groups approaching the Ti dopant.

In conclusion, we have used first-principles methods and neutron inelastic scattering to study pure and Ti-doped sodium alanate ($NaAlH_4$), a material that holds great promise for reversible hydrogen storage. The total energy calculations indicate that substitutional Ti doping in $NaAlH_4$ is energetically stable. We find that the dopant prefers to substitute for Na and attracts several hydrogen atoms, softening and breaking the corresponding Al-H bonds. We also find it energetically favorable for the Ti to drag extra H atoms into the system. These results point to an interesting direction for future research, namely, the possibility of producing a material, sodium-titanium alanate, that might benefit from the ability of Ti to accommodate extra hydrogens in its vicinity and thus exhibit improved H-storage capabilities.

[1] B. Bogdanovic and M. Schwickardi, J. Alloys Compd. **253**, 1 (1997).

[2] K. J. Gross, G. J. Thomas, and C. M. Jensen, J. Alloys Compd. **330–332**, 683 (2002).

[3] T. Kiyobayashi, S. S. Srinivasan, D. Sun, and C. M. Jensen, J. Phys. Chem. A **107**, 7671 (2003).

[4] G. J. Thomas, K. J. Gross, N. Y. C. Yang, and C. M. Jensen, J. Alloys Compd. **330–332**, 702 (2002).

[5] D. Sun, T. Kiyobayashi, H. T. Takeshita, N. Kuriyama, and C. M. Jensen, J. Alloys Compd. **337**, L8 (2002).

[6] G. Sandrock, K. Gross, and G. Thomas, J. Alloys Compd. **339**, 299 (2002).

[7] R. A. Zidan, S. Takara, A. Hee, and J. M. Jensen, J. Alloys Compd. **285**, 119 (1999).

[8] J. Huot, S. Boily, V. Guther, and R. Schultz, J. Alloys Compd. **283**, 304 (1999).

[9] J. R. D. Copley, D. A. Neumann, and W. A. Kamitakahara, Can. J. Phys. **73**, 763 (1995).

[10] J. P. Perdew, K. Burke, and M. Ernzerhof, Phys. Rev. Lett. **77**, 3865 (1996).

[11] X. Gonze *et al.*, Comput. Mater. Sci. **25**, 478 (2002). See also http://www.abinit.org

[12] N. Troullier and J. L. Martins, Phys. Rev. B **43**, 1993 (1991).

[13] M. Fuchs and M. Scheffler, Comput. Phys. Commun. **119**, 67 (1999).

[14] S. Baroni, S. de Gironcoli, A. Dal Corso, and P. Giannozzi, Rev. Mod. Phys. **73**, 515 (2001).

[15] G. L. Squires, *Introduction to the Theory of Thermal Neutron Scattering* (Dover, New York, 1996).

[16] V. K. Bel'skii, B. M. Bulychev, and A. V. Golubeva, Acta Crystallogr., Sect. B: Struct. Crystallogr. Cryst. Chem. **24**, 1968 (1982).

[17] B. C. Hauback, H. W. Brinks, C. M. Jensen, K. Murphy, and A. J. Maeland, J. Alloys Compd. **358**, 142 (2003).

[18] V. Ozolins, E. H. Majzoub, and T. J. Udovic, J. Alloys Compd. **375**, 1 (2004).

[19] B. Bogdanovic, R. A. Brand, A. Marjanovic, M. Schwickardi, and J. Tolle, J. Alloys Compd. **302**, 36 (2000).

[20] J. Íñiguez, T. Yildirim, and T. J. Udovic (unpublished).

[21] T. Yildirim, Chem. Phys. **261**, 205 (2000).

[22] K. J. Gross, G. Sandrock, and G. J. Thomas, J. Alloys Compd. **330–332**, 691 (2002).